Synthesis of Aerodynamic Transfer Functions for Elastic Flight Vehicles

Jack Morito Ii*
The Boeing Company, Seattle, Wash.

This paper presents a method of generating the reasonable approximations to aerodynamic transfer functions on general configurations of elastic wings or wing-body combinations. The transfer functions are specified by asymptotic expansions in which either the polynomial or rational function approximation is applied. Procedures are described for incorporating a variety of quantitative and qualitative information concerning the unsteady aerodynamic behavior in both subsonic and supersonic flow regimes. Two types of power series approximations, power series with real coefficients and the other with complex coefficients, are applied. Consideration of the hereditary effect of wake vortices on the wing-bound vortices and the analogy with the behavior of a feedback control system provide useful guidance in selecting the form of approximation in both subsonic and supersonic flows. By relaxing the restriction imposed in the first-order piston theory, a limit as $\omega \to \infty$ is discussed. Both the standard and extended Padé approximants $s=0$ and $s=R$ are studied in order to improve their accuracy at high k values. The above procedures are programmed in conjunction with the lifting surface theory, doublet lattice, and advanced Mach box scheme and demonstrated for the determination of AGARD wing aerodynamics and the flutter stability boundary for advanced aircraft configurations. The results appear to be satisfactory.

Nomenclature

a = speed of sound
a_j, b_j, d_j = coefficients of power series
A_j, B_j, D_j = coefficients of extended Padé approximant
b or b_0 = reference dimension, unit box side or wing root semichord
$B(k)$ = real part of a complex function
$C(k)$ = imaginary part of a complex function
$\{f\}$ = sequence of functions
i = unit of imaginaries, $\sqrt{-1}$
k = reduced frequency, $\omega b/U$
M = Mach number, U/a
q = dynamic pressure, $\frac{1}{2}\rho U^2$
q_{ij} = generalized force in which the pressure is for the jth mode and the deflection is due to the ith mode
s = complex variable in frequency domain, $s=ik=i\omega b/U$
U = freestream velocity
u,v,w = backwash, sidewash, and upwash velocity components
$w(t)$ = local velocity on piston surface
x,y,z = reference coordinate system: x positive aft, y positive right, z positive upward.
ξ,η,ζ = dummy variables of integration
$\Gamma(t)$ = circulation
γ = strength of bound vortices and ratio of specific heats, C_p/C_v
ω = frequency

Subscripts and Superscripts

a = quantity related to airfoil
i,j = indices of series expansion and modal displacement
i = input
o = output
s = quantity related to shed vortices
∞ = condition at infinity

Presented as Paper 77-452 at the AIAA Dynamics Specialist Conference, San Diego, Calif., March 24-25, 1977; submitted May 5, 1977; revision received July 12, 1978.

Index categories: Nonsteady Aerodynamics; Subsonic Flow; Aeroelasticity and Hydroelasticity.

*Research Specialist. Member AIAA.

Introduction

THIS paper presents a method of generating the reasonable approximations to aerodynamic transfer functions on general configurations of elastic wings or wing-body combinations. The transfer functions are specified by asymptotic expansions in which either the polynomial or rational function approximation is applied. The direct representation of aerodynamic transfer functions by applying both the strip and two-dimensional lifting surface theories will be done in a straightforward manner.[1,2] The exact aerodynamic loads on general three-dimensional wings which are represented by the Fredholm-type integral equation, are extremely tedious. Furthermore, these exact solutions are not analytically obtainable and hence these are only approximations.

Two types of power series approximations can be specified: power series with real coefficients and the other with complex coefficients. From the practical point of view, the real coefficient power series method is applied in this paper.[1,3-5] The discussion will be extended to finding the "best" curve which represents data which are subject to error and inaccuracy because of the numerical procedure used in evaluating the unsteady aerodynamic loadings or error in the flight and wind tunnel experimental data. The least-squares approximation and ordinary curve fit method are applied.

From the study of unsteady aerodynamic behavior in the subsonic flow regime, there exists an interaction between the wing-bound vortices and its floating-wake vortices. In this flowfield, the system loop is closed and a form of the rational function is believed to be best suited. In the supersonic flowfield, even when the wing trailing edge is subsonic, any disturbance caused by the wake vortices cannot influence the original time-dependent singularities. Thus, in this flowfield, the system loop is opened and the appropriate form of the transfer function should be polynomial.

In the limiting case of the reduced frequency $k \to \infty$ (or the flow Mach number is large), the influence of the pressure variation is only local so that piston theory may be applied. Under this condition the higher-order piston theory is necessary and is a form of asymptotic power series expansion in s because a ratio between the local velocity $w(t)$ and local speed of sound is not small.[7] Thus, the form of polynomial in s in the supersonic flow is acceptable even in this extreme condition.

One of the rational functions in the transformed frequency domain conveniently applies the Padé approximant in the subsonic flow regime.[2,6,8] Since the Padé approximant is constructed around $s=0$ and the quantitative error is magnified as s increases, the extended Padé approximants at $s=R$ are formulated in order to improve their accuracy at the high k values.

The initial points of both polynomials and rational functions are usually steady aerodynamic values at $ik=0$ for the given modes. If the test data are known accurately at one end of the curve ($s=0$), the curve passes exactly through this point. The program, however, allows the best approximate fit at the initial point of a set of data, if the test data at $s=0$ are not available.

The above procedures are programmed in conjunction with the lifting surface theory,[10,15] doublet lattice,[11,12,15] and advanced Mach box scheme,[13-15] and then demonstrated for an AGARD wing for the flowfield range from $M=0$ to 2.0. Determination of flutter stability boundaries for an advanced SST is also examined by applying this method.

Asymptotic Expansions for General Complex Functions Around Finite Points

For the vibrational and flutter analysis, the aerodynamic loadings are usually computed in a harmonic motion which is a function of $ik=s$.

Consider the following function specified by the q asymptotic expansions:

$$\begin{aligned} F[\xi(k)+i\eta(k)] &= B(k)+iC(k) \\ &\underset{k\to k_i}{\sim} \sum_{j=0}^{N_i} a_j(i)(k-k_i)^j + E_{ni}(k-k_i) \\ &\underset{k\to k_i}{\sim} (k-k_i)^{P+N_i} \sum_{j=0}^{N_i} a_{N_i-j}(k-k_i)^{-j} + E_{ni}{}^{(I-P)}(k-k_I) \\ &(i=1,2,3,\ldots q) \end{aligned} \tag{1}$$

where $k_i<k_{i+1}$, $E_{ni}(\ )$ and $E_{ni}{}^{(1-P)}(\ )$ are $(k-k_i)^{N_i+1}$ and $(k-k_i)^{1-P}$, respectively, and P is an integer but otherwise unknown.

Equation (1) can be expanded about the points $k_1, k_2, \cdots, k_q$ and this problem statement is valid provided that the expansion point k_q is finite. Particular interest is given to expansion about zero and infinity which is obtained by $1/k\to 0$. In a particular problem, the expansion about zero is essential.

Expansion About Zero with Complex Coefficients

Assume that for a range of values of k of interest about zero, the function F can be approximated in the following polynomial:

$$F[\xi(k),\eta(k)] = B(k)+iC(k) \sim \sum_{j=0}^{N} a_j{}^{(0)} k^j + E_{n0}(k) \tag{2}$$

and

$$a_j{}^{(0)} = b_j{}^{(0)} + ic_j{}^{(0)}$$

where $b_j{}^{(0)}$ and $c_j{}^{(0)}$ are real coefficients. Then, the real and imaginary parts of F are approximated by

$$B(k) = \sum_{j=0}^{N} b_j{}^{(0)} k^j \tag{3a}$$

$$C(k) = \sum_{j=0}^{N} c_j{}^{(0)} k^j \tag{3b}$$

In Eqs. (3), if the number of k values $n=N+1$, the unknown coefficients b_j and c_j are determined. However, if $n>N+1$, Eqs. (3) are an overdetermined set of linear equations which can be satisfied only approximately. For simplicity, the superscript (0) is removed.

The set of Eqs. (3) can be written in matrix form as follows:

$$[K]\{b_N\} = \{B(k_n)\} \tag{4a}$$

$$[K]\{c_N\} = \{C(k_n)\} \tag{4b}$$

where $[K]$ is an $n\times(N+1)$ matrix and

$$[K] = \begin{bmatrix} 1 & k_1 & k_1^2 & k_1^3 & \cdots & k_1^N \\ 1 & k_2 & k_2^2 & k_2^3 & \cdots & k_2^N \\ & & & \cdots & & \\ 1 & k_n & k_n^2 & k_n^3 & \cdots & k_n^N \end{bmatrix}$$

Thus,

$$\{b_N+ic_N\} = [K]^{-1}\{B(k_n)+iC(k_n)\} \tag{5}$$

In the transformed frequency domain,

$$\bar F(s) = \bar F(ik) = \sum_{j=0}^{N} i^{-j}(b_j+ic_j)s^j$$

Therefore, the matrix of the coefficients of the Nth order polynomial becomes a complex matrix.

Expansion About Zero with Real Coefficients

Instead of complex coefficients, the function F can be approximated by a polynomial in $s=ik$ with real coefficients,

$$\bar F(s) = a_0 + a_1(ik) + a_2(ik)^2 + \cdots a_N(ik)^N = B(k)+iC(k) \tag{6}$$

in which N is usually taken as an odd number which produces equal numbers of terms in the real and imaginary parts of $\bar F(s)$. Thus,

$$[K_{2n}]\{a_{2n}\} = \{B(k)\}$$

$$[K_{2n+1}]\{a_{2n+1}\} = \{C(k)\}$$

Solving for each coefficient

$$\{a_{2n}\} = [K_{2n}]^{-1}\{B(k)\} \tag{7a}$$

$$\{a_{2n+1}\} = [K_{2n+1}]^{-1}\{C(k)\} \tag{7b}$$

where

$$[K_{2n}] = \begin{bmatrix} 1 & -k_1^2 & k_1^4 & \cdots & (i)^{N-1} & k_1^{N-1} \\ 1 & -k_2^2 & k_2^4 & \cdots & (i)^{N-1} & k_2^{N-1} \\ & & & \cdots & & \\ & & & \cdots & & \\ 1 & -k_M^2 & k_M^4 & \cdots & (i)^{N-1} & k_M^{N-1} \end{bmatrix} \tag{8}$$

and

$$[K_{2n+1}] = \begin{bmatrix} k_1 & -k_1^3 & k_1^5 & \cdots & (i)^{N-1} & k_1^N \\ k_2 & -k_2^3 & k_2^5 & \cdots & (i)^{N-1} & k_2^N \\ & & & \cdots & & \\ k_M & -k_M^3 & k_M^5 & \cdots & (i)^{N-1} & k_M^N \end{bmatrix} \tag{9}$$

It is noticed that if $M>(N+1)/2$ the linear equations consist of an overdetermined set.

In our problem, the coefficient a_0 is usually known and is equivalent to a steady-state value, $B(0)$. In this case, the computed curves in the s plane must pass through the values at $k=0$. Therefore,

$$\{a_{2n}\}_{n\neq 0}=[K_{2n}]^{-1}_{k\neq 0}\{\{B(k)\}-\{B(0)\}\} \tag{10a}$$

$$\{a_{2n+1}\}_{n\neq 0}=[K_{2n+1}]^{-1}_{k\neq 0}\{C(k)\}_{k\neq 0} \tag{10b}$$

where $[K_{2n}]_{k\neq 0}$ and $[K_{2n+1}]_{k\neq 0}$ are obtained by deleting the first row and column from the matrices of Eqs. (8) and (9), and

$$\{\{B(k)\}-\{B(0)\}\}=\begin{Bmatrix} B(k_2)-B(0) \\ B(k_3)-B(0) \\ \cdots \\ \cdots \\ B(k_M)-B(0) \end{Bmatrix}$$

From a practical point of view, the real coefficient expansion is applied in this study.[1,3-5] In the case of an overdetermined set of data, the numerical fit method is applied in finding the "best" curves.

Characteristic Behavior of Unsteady Aerodynamics of an Oscillatory Thin Airfoil

Subsonic Flowfield

In order to investigate the characteristic behavior of unsteady aerodynamics of an airfoil, a two-dimensional thin wing in incompressible flow is considered for the sake of simplicity, as shown in Fig. 1. In this flowfield, the velocity potential is governed by

$$\nabla^2\phi=0$$

The boundary conditions are time-dependent and

$$\phi_t+P/\rho+q^2/2=F(t)$$

with the infinite upstream condition

$$F(t)=U^2/2+P_\infty/\rho_\infty=\text{constant}$$

In inviscid flow, from Kelvin's theorem,

$$\frac{D\Gamma(t)}{Dt}=\frac{D}{Dt}(\Gamma_a(t)+\Gamma_s(t))=0 \tag{11}$$

where

$$\Gamma_a(t)=\int_{-b_0}^{b_0}\gamma(\xi,t)\mathrm{d}\xi \qquad \Gamma_s(t)=\int_{b_0}^{\infty}\epsilon(\xi,t)\mathrm{d}\xi$$

Thus, $\Gamma_a(t)+\Gamma_s(t)=$constant and at $t=0^-$, there is no circulation, then

$$\Gamma_a(t)=-\Gamma_s(t) \tag{12}$$

From this well-known fact, the shed vortices at any time influence the instantaneous airfoil vortices which is extremely similar to the closed loop having feedback as shown in Fig. 2.

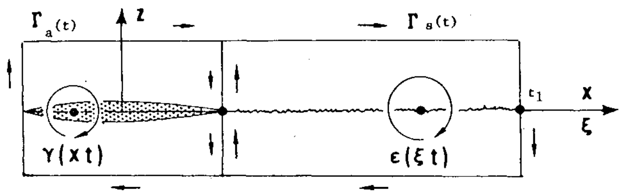

Fig. 1 Two-dimensional airfoil bound and shed vortices in a finite wake regime.

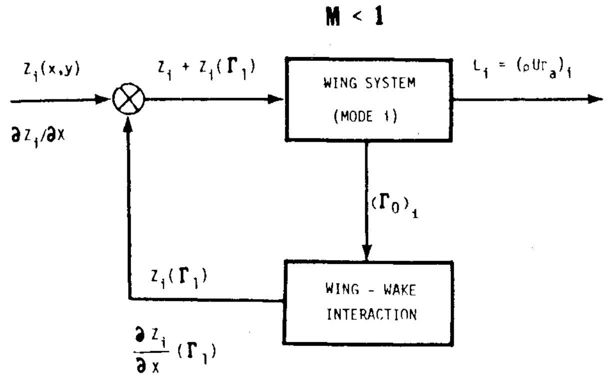

Fig. 2 Schematic block diagram of wing system in subsonic flow: $z_i(x,y)$ is the translational displacement of mode i; $\partial z_i(x,y)/\partial x$ is the angular displacement of mode i; $z_i(\Gamma_1)$ is the translational displacement of mode i caused by the hereditary effect from the wake vortices; $\partial z_i/\partial x(\Gamma_1)$ is the angular displacement of mode i caused by the hereditary effect from the wake vortices.

In order to investigate the feedback effect of the shed vortices, the wing-bound vortices are split up by

$$\gamma_a(x,t)=\gamma_0(x,t)+\gamma_1(x,t) \tag{13}$$

where $\gamma_0(x,t)$ is the quasi-steady vortex whose strength is required at anytime to produce the upwash distribution over the airfoil prescribed by the given modes of motion, assuming that no wake is present and $\gamma_1(x,t)$ is the wake-effected vortex whose distributed strength cancels the upwash due to the wake vortices, leaving the tangency and Kutta-Jukowsky conditions undisturbed.

From thin airfoil theory

$$\gamma_0(x,t)=\frac{2}{\pi}\left(\frac{b_0-x}{b_0+x}\right)^{\frac{1}{2}}P\int_{-b_0}^{b_0}w_0(\xi,0,t)\left(\frac{b_0+\xi}{b_0-\xi}\right)^{\frac{1}{2}}\frac{\mathrm{d}\xi}{x-\xi} \tag{14}$$

where

$$w_0(x,0,t)\simeq\frac{DZ_c(x,t)}{Dt}\simeq\frac{\partial Z_c}{\partial x}+U\frac{\partial Z_c}{\partial x} \tag{15}$$

In a similar manner

$$\gamma_1(x,t)=\frac{2}{\pi}\left(\frac{b_0-x}{b_0+x}\right)^{\frac{1}{2}}P\int_{-b_0}^{b_0}w_1(\xi,0,t)\left(\frac{b_0+\xi}{b_0-\xi}\right)^{\frac{1}{2}}\frac{\mathrm{d}\xi}{x-\xi} \tag{16}$$

where $w_1(\xi,0,t)$ is the upwash induced by the wake

$$-w_{\text{wake}}(\xi,0,t)=\frac{1}{2\pi}\int_{b_0}^{\infty}\frac{\epsilon(\xi_1,t)}{\xi-\xi_1}\mathrm{d}\xi_1 \tag{17}$$

and P denotes the Cauchy principal value of the improper integral. Thus, the circulation on the airfoil caused by the

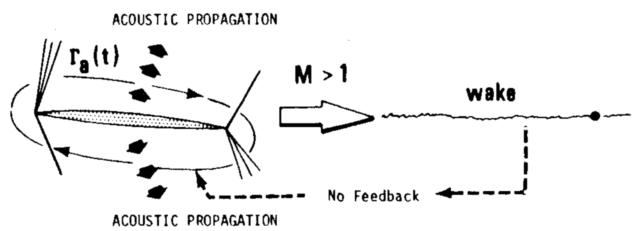

Fig. 3 Two-dimensional wing in supersonic flow.

wing-wake interaction is

$$\Gamma_I(t)=\int_{-b_0}^{b_0}\gamma_I(x,t)\mathrm{d}x=\frac{1}{\pi^2}\int_{-b_0}^{b_0}\sqrt{\frac{b_0-x}{b_0+x}}\,\mathrm{d}x$$
$$\times P\int_{-b_0}^{b_0}\sqrt{\frac{b_0+\xi}{b_0-\xi}}\,\frac{\mathrm{d}\xi}{x-\xi}\int_{b_0}^{\infty}\frac{\epsilon(\xi_I,t)}{\xi-\xi_I}\mathrm{d}\xi_I \tag{18}$$

By applying Glauert integral formula, Eq. (18) can be integrated:

$$\Gamma_I(t)=\int_{b_0}^{\infty}\epsilon(\xi_I,t)\left[\sqrt{\frac{\xi_I+b_0}{\xi_I-b_0}}-1\right]\mathrm{d}\xi_I \tag{19}$$

which is the wing circulation fed back from the wake vortices which are produced by the prior wing motion.

In the subsonic flowfield the feedback mechanism is carried out by propagation at the speed of sound, a. The characteristic nature of feedback is similar to the incompressible case in which a is infinite.

In the oscillatory case whose angular frequency is ω,

$$\epsilon(x,t)=-\frac{1}{U}\Gamma_a'\left(t-\frac{x-b_0}{U}\right)=g\exp\left[i\omega\left(t-\frac{x-b_0}{U}\right)\right]$$
$$=g\exp\left[ik_0\left(\tau-\frac{x}{b_0}+1\right)\right] \tag{20}$$

where $\Gamma_a'=\partial\Gamma_a/\partial t$, $k_0=b_0/U$, and τ is the dimensionless time $=Ut/b_0$. Substitution of Eq. (20) into Eq. (19) yields

$$\Gamma_I(\tau)=-b_0ge^{-ik_0}\left[K_0(ik_0)+K_I(ik_0)+e^{-ik_0}/ik_0\right]e^{ik_0\tau} \tag{21}$$

provided that the limit value of Eq. (19) as $\xi_I\to\infty$ may vanish. K_ν is the modified Bessel function of the second kind and order ν. Therefore, the nontime-dependent part of the feedback circulation can be expressed in the transformed frequency domain as

$$\bar{\Gamma}(s)=-b_0ge^{-s}\left[K_0(s)+K_I(s)+e^{-s}/s\right] \tag{22}$$

In Eq. (22). the modified Bessel functions can be expanded by ascending series in s. Thus, the feedback circulation of a two-dimensional wing can be easily expanded by a general power series in s. By analogy to the operational mathematics, the schematic block diagram of the oscillating lifting surface in the subsonic flow can be synthesized as shown in Fig. 2.

Supersonic Flowfield

In supersonic flow in which the flow velocity exceeds the speed of acoustic propagation, the unsteady aerodynamic behavior is completely different from that in subsonic flow.

As illustrated in Fig. 3, the singularities of the original wing cannot be influenced by their wakes. This phenomenon can be extended to a three-dimensional wing whose trailing edge is subsonic. Therefore, in supersonic flow any singularities over the wing cannot be influenced by their own floating singularities. Thus, in this flowfield the system loop circuit is open as illustrated in Fig. 4 and rational functions are not necessary in supersonic flow.

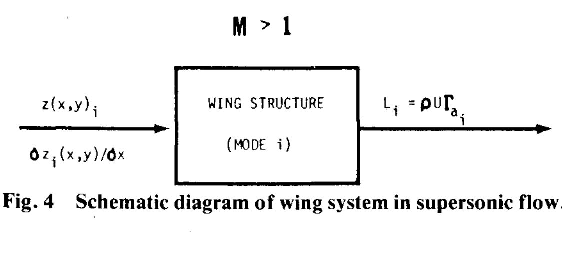

Fig. 4 Schematic diagram of wing system in supersonic flow.

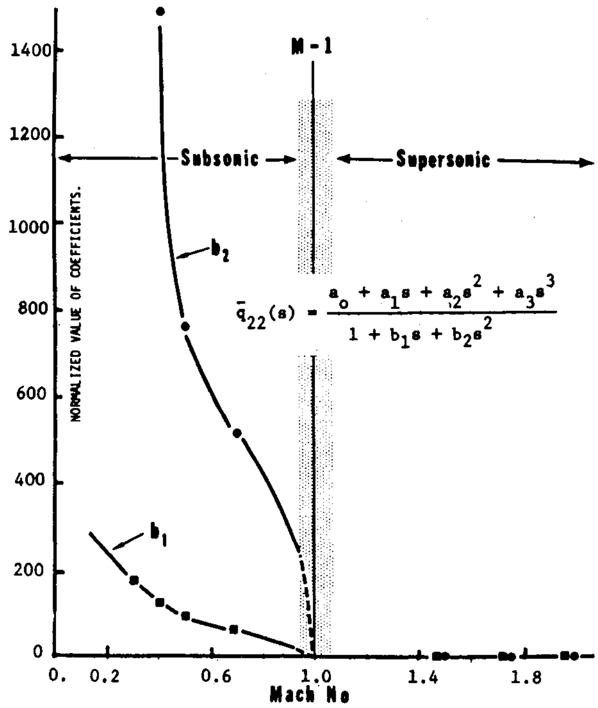

Fig. 5 Normalized coefficients b_1 and b_2 vs flow Mach number.

The above statement can be demonstrated by the numerical examples tabulated in Tables 1-8 in Ref. 2. In this case, the Padé approximant [2, 3] is applied for both subsonic and supersonic flows as a form of

$$\bar{q}_{22}(s)=\frac{a_0+a_1s+a_2s^2+a_3s^3}{1+b_1s+b_2s^2} \tag{23}$$

The coefficients of the terms of s and s^2 in the denominator, which are normalized by the constant term in the denominator to be unity, are plotted against the flow Mach numbers as shown in Fig. 5. After passing over the sonic line of $M=1$, the values of these coefficients become very small compared to the ones of subsonic flow as discussed in the previous statement.

Limit Cases as $\omega\to\infty$ and $\omega\to 0$

In the limit of very high speed or $\omega\to\infty$, the influence of the singularity variation (or pressure variation) is only local. Thus, piston theory is a satisfactory approximation.

Consider a piston moving with a velocity $w(t)$ in the end of a channel containing perfect gas as illustrated in Fig. 6. Provided that the piston generates only simple waves and produces no entropy changes, the exact pressure expression for the instantaneous pressure $p(t)$ on the piston surface is[7]

$$\frac{p(t)}{p_\infty}=\left[1+\frac{\gamma-1}{2}\frac{w(t)}{a_\infty}\right]^{2\gamma/(\gamma-1)} \tag{24}$$

By expanding Eq. (24) by the binominal theorem, the pressure difference Δp is obtained as

$$\Delta p(t)=p-p_\infty=\frac{\rho_\infty a^2}{\gamma[p(t)/p_\infty-1]}$$
$$=\rho_\infty a_\infty^2\left[\frac{w(t)}{a_\infty}+\frac{\gamma+1}{4}\left(\frac{w(t)}{a_\infty}\right)^2+\frac{\gamma+1}{12}\left(\frac{w(t)}{a_\infty}\right)^3\right.$$
$$\left.\cdots+\frac{[2\gamma/(\gamma-1)]!}{\gamma[2\gamma/(\gamma-1)-r]r!}\left(\frac{\gamma-1}{2}\right)^r\left(\frac{w(t)}{a_\infty}\right)^r+\cdots\right] \tag{25}$$

Since $\omega\to\infty$ and $w(t)/a_\infty$ is not small, the successive power series cannot be neglected.

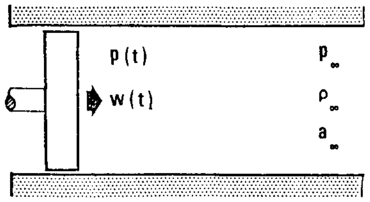

Fig. 6 One-dimensional piston in channel.

Now, the lifting surface motion is described by

$$z(x,y,t) = z_0(x,y)e^{i\omega t}$$

then

$$\frac{w(t)}{U} = \left[\frac{ik_0 z_0(xy)}{b_0} + \frac{\partial z_0}{\partial x}\right]e^{i\omega t}$$

Therefore, the dimensionless pressure difference in the transformed s plane is

$$\frac{\Delta p(s)}{q_\infty} = \frac{2}{M^2}\left[M\left(\frac{sz_0}{b_0} + \frac{\partial z_0}{\partial x}\right) + \frac{(\gamma+1)M^2}{4}\left(\frac{sz_0}{b_0} + \frac{\partial z_0}{\partial x}\right)^2 + \frac{(\gamma+1)M^3}{12}\left(\frac{sz_0}{b_0} + \frac{\partial z_0}{\partial x}\right)^3 + \cdots\right]$$

$$= a_0 + a_1 s + a_2 s^2 \cdots = \sum_{j=0}^{\infty} a_j s^j \tag{26}$$

where

$$a_0 = \frac{2z_0'}{M}\left[1 + \frac{(\gamma+1)}{4}z_0' + \frac{(\gamma+1)M^2}{12}(z_0')^2 + \cdots\right]$$

$$a_1 = \frac{2z_0}{Mb_0}\left[1 + \frac{(\gamma+1)M}{2}z_0' + \frac{(\gamma+1)M^2}{4}(z_0')^2 + \cdots\right]$$

$$a_2 = \cdots$$

If the thickness $z_\tau(x,y)$ and the camber $z_M(x,y)$ are accounted, the similar form of Eq. (26) can be obtained. The lift force which is $\Delta p_L - \Delta p_U$ can be expanded in the similar polynomial with respect to s.

By analogy with the behavior of a feedback control system, in the limit as $\omega \to 0$ the system loop is open and only the steady-state aerodynamics remains.

Subsonic flow

$$\lim_{s\to 0}\sum_{j=0} a_j s^j \Big/ \left[1 + \sum_{j=1} b_j s^j\right] = a_0 = q_{ij}(0,M) \tag{27}$$

Supersonic flow

$$\lim_{s\to 0} a_j s^j = a_0 = q_{ij}(0,M) \tag{28}$$

Construction of Rational Functions at $s=0$ and $s=R$

The Fredholm-type integral equation of either first or second kind with a completely continuous kernel in the specified domain of S in L^2 can be expandable in a sequence of power series expansions. Thus, the generalized aerodynamic forces, which are the integrated values of a product of power series in which the modal functions are assumed to be expandable in power series also, are also shown in a sequence of power series.

Construction of rational functions can be performed by the Padé approximant $[m,n]$ in which $n = m+1$ by

$$q_{ij}(s,M) = \sum_{j=0}^{n} a_j s^j \Big/ \left[1 + \sum_{j=1}^{m} b_j s^j\right] \tag{29}$$

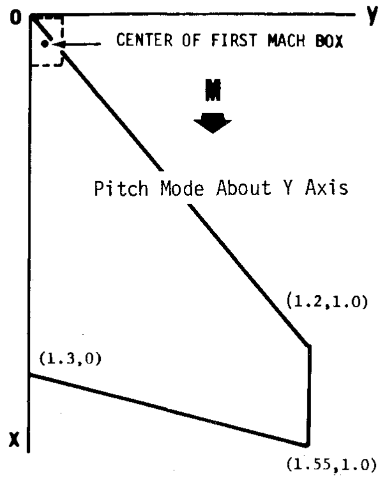

Fig. 7 AGARD wing tested.

From the previous polynomial approximation, $q_{ij}(s,M)$ can be expressed by the Maclaurin series in which $N = n+m$:

$$F_{ij}(s,M) = \sum_{k=0}^{N} d_k s^k \tag{30}$$

The Padé approximant, Eq. (29), is usually constructed at $s=0$, and then the quantitative error is magnified as s increases. Therefore, for the large value of k's the need exists to construct the Padé approximant at an arbitrary value of $s=R$. A linear transformation $s = s' + R$ is intended. Then the original polynomial is expanded by

$$F(s) = F(s') = \sum_{j=0}^{N} d_j(s'+R)^j = \sum_{j=0}^{N} D_j s'^j \tag{31}$$

and the extended Padé approximant[9] will be

$$Q_{ij}(s',M) = \sum_{j=0}^{n} A_j s'^j \Big/ \left(1 + \sum_{j=1}^{m} B_j s'^j\right) \tag{32}$$

Table 1 Coefficients of seventh-order polynomials (mode 1 = pitch, mode 2 = translation, Mach number = 0.4)

$$q_{ij}(s,M) = d_{i,j,0} + d_{ij,1}s + d_{ij,2}s^2 + d_{ij,3}s^3 + d_{ij,4}s^4 + d_{ij,5}s^5 + d_{ij,6}s^6 + d_{ij,7}s^7$$

Coefficient $d_{ij,n}$	Mode i	Mode j 1 Real	1 Imaginary	2 Real	2 Imaginary
$d_{ij,0}$	1	−1.817470	0.0	0.0	0.0
	2	−2.368620	0.0	0.0	0.0
$d_{ij,1}$	1	−5.7310170	0.0	−3.2382106	0.0
	2	−6.4656011	0.0	−4.2545654	0.0
$d_{ij,2}$	1	−2.9131017	0.0	−2.8173991	0.0
	2	−2.8819796	0.0	−2.9647951	0.0
$d_{ij,3}$	1	0.0719199	0.0	−0.0690546	0.0
	2	0.0480197	0.0	−0.1063979	0.0
$d_{ij,4}$	1	−0.0162258	0.0	0.0665529	0.0
	2	−0.0285799	0.0	0.0624804	0.0
$d_{ij,5}$	1	−0.0314881	0.0	−0.0666203	0.0
	2	−0.0312098	0.0	−0.0717336	0.0
$d_{ij,6}$	1	0.0039190	0.0	0.0096378	0.0
	2	0.0035508	0.0	0.0101161	0.0
$d_{ij,7}$	1	−0.0022104	0.0	−0.0039403	0.0
	2	−0.0023107	0.0	−0.0043641	0.0

Table 2 Coefficients of 4/3-order Padé approximants (mode 1 = pitch, mode 2 = translation)

$$q_{ij}(s,M)=\frac{a_{ij,0}+a_{ij,1}s+a_{ij,2}s^2+a_{ij,3}s^3+a_{ij,4}s^4}{1+b_{ij,1}s+b_{ij,2}s^2+b_{ij,3}s^3}$$

Coef- ficient	Mode i	Mode j 1 Real	1 Imaginary	2 Real	2 Imaginary
$a_{ij,0}$	1	−1.817	0.0	0.0	0.0
	2	−2.369	0.0	0.0	0.0
$a_{i,j,1}$	1	−5.950	0.0	−3.238	0.0
	2	−6.789	0.0	−4.255	0.0
$a_{ij,2}$	2	−3.516	0.0	−3.144	0.0
	2	−3.654	0.0	−3.460	0.0
$a_{ij,3}$	1	0.022605	0.0	−0.1455	0.0
	2	−0.013259	0.0	−0.1904	0.0
$a_{ij,4}$	1	0.2069	0.0	0.3042	0.0
	2	0.1962	0.0	0.3153	0.0
$b_{ij,1}$	1	0.1206	0.0	0.1009	0.0
	2	0.1365	0.0	0.1165	0.0
$b_{ij,2}$	1	−0.048658	0.0	−0.064213	0.0
	2	−0.046634	0.0	−0.061425	0.0
$b_{ij,3}$	1	−0.012682	0.0	−0.019688	0.0
	2	−0.012960	0.0	−0.019536	0.0

Numerical Examples

The above procedures are programmed and written for the CDC 6600 in conjunction with the lifting surface theory,[10,15] doublet lattice,[11,12,15] and advanced Mach box scheme.[13-18] The maximum modal size of the presently designed program is 40×40 for polynomials and 20×20 for Padé approximants. The maximum degree of the approximating polynomials is 11,

An AGARD wing illustrated in Fig. 7 is tested for an actual application. The flowfields tested range from $M=0$ to 2.0 and the reduced frequencies which are based on the semiroot chord are chosen from 0 to 3.0. Construction of polynomials and Padé approximants is performed for both seventh-degree power series in s which are approximated by 4/3 Padé fractions and ninth-degree power series in s which are approximated by 5/4 Padé fractions.

Computed results for seventh-degree polynomials at $M=0.4$ are shown in Table 1 and the Padé approximants of 4/3 degree at $R=0$ for the identical condition are shown in

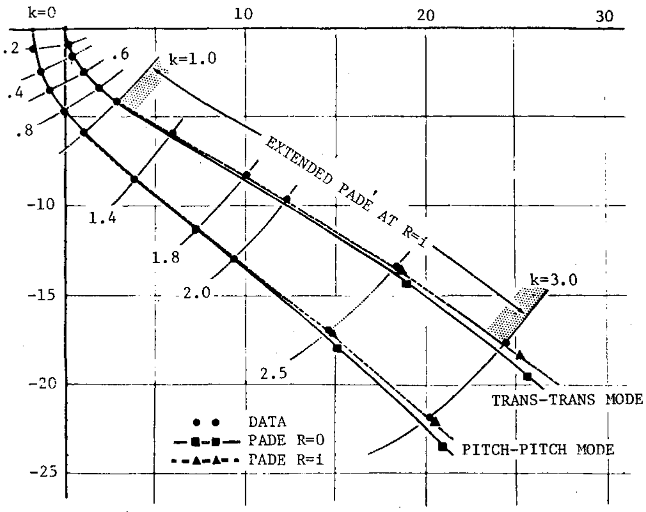

Fig. 8 Padé approximants at $R=0$ and $R=i$, $M=0.4$, modes 1-1 and 2-2.

Table 2. The extended Padé approximants at $R=i$ for the above condition are shown in Table 3. Mode 1 is pitching about the wing apex and mode 2 is translation along the z axis.

Figure 8 illustrates the transformed aerodynamics represented by Padé approximants both at $R=0$ and $R=i$. From these curves, as the k value increases the Padé approximants constructed at $R=0$ increase their quantitative error. The extended Padé approximants may improve their accuracy, but in this example, the improvement is modest because the range of k and the extended value R are not large enough.

Figure 9 shows seventh-degree polynomials in the pitch-pitch mode against various subsonic Mach numbers. Figure 10 shows ninth-degree polynomials in the same condition. These figures show a comparison with the data points which are evaluated from the subsonic lifting surface theory. These curves show excellent fit with these data points and the deviation from the given data points is extremely small even though the polynomials are seventh-degree.

Computed results for seventh-degree polynomials at $M=1.75$ are shown in Table 4. Figure 11 shows seventh-degree polynomials in the pitch-pitch mode for various

Table 3 Coefficients of extended Padé approximants (Mach number = 0.4, $R=i$)

Coefficient	Mode i	Mode j 1 Real	1 Imaginary	2 Real	2 Imaginary
$a_{ij,0}$	1	1.075487	5.832215	2.874314	−3.23184
	2	0.481229	−6.542520	3.017159	−4.21554
$a_{ij,1}$	1	−5.513873	−4.065690	−4.223498	−4.53074
	2	−5.822699	−3.876341	−5.314243	−4.25176
$a_{ij,2}$	1	−0.937046	1.733686	−2.163314	2.75909
	2	−0.666641	1.492033	−1.874775	−3.20006
$a_{ij,3}$	1	1.315542	0.566975	1.959039	0.97932
	2	1.244283	0.559479	2.310746	1.14964
$a_{ij,4}$	1	0.324559	0.1241974	0.474808	−0.19424
	2	0.282994	0.1513599	0.512338	−0.21261
$b_{ij,1}$	1	−0.259693	0.1464569	−0.363025	0.04843
	2	−0.255981	0.1604917	−0.410841	0.04479
$b_{ij,2}$	1	−0.126370	−0.0798531	−0.163057	−0.036118
	2	−0.117667	−0.0892365	−0.169514	−0.047699
$b_{ij,3}$	1	−0.0032018	0.0091296	−0.009662	0.030177
	2	−0.0010279	0.0089882	−0.006309	0.034330

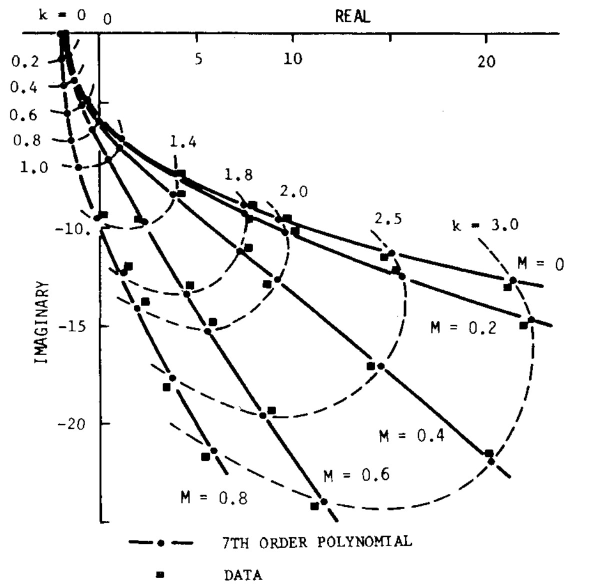

Fig. 9 q_{11} from lifting surface theory and from seventh-order polynomial approximation for $0 \leq k \leq 3.0^+$ and various subsonic Mach numbers.

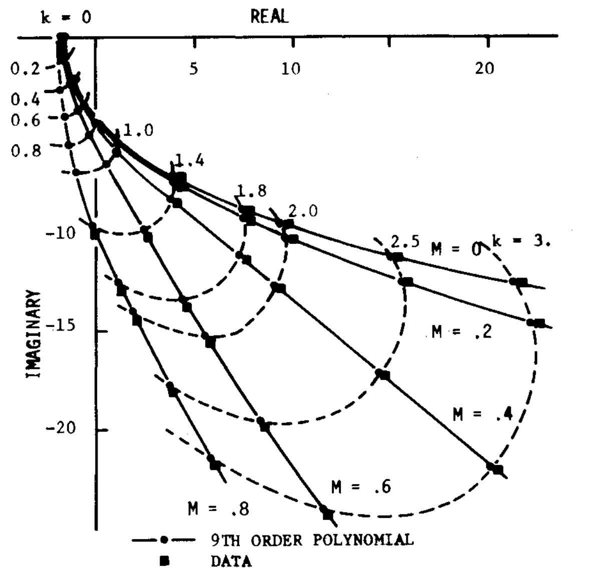

Fig. 10 q_{11} from lifting surface theory and from ninth-order polynomial approximation for $0 \leq k \leq 3.0^+$ and various subsonic Mach numbers.

supersonic Mach numbers. In contrast to subsonic flow, the variation in the real part with increasing s is very small compared to the change in the imaginary part. Since the wing is oscillating about the y axis, time delay due to the speed of sound in the flowfield is almost linearly proportional to the reduced frequency. The real parts of airloads, however, are so little influenced by the floating vortices that they are almost constant.

The analysis is extended to the flutter studies to include an active control surface driven by a flutter-suppression system.[16] Figure 12 illustrates an arrow wing SCAR configuration used in this test.

Figure 13 illustrates the locations of roots (root loci) with altitude varied from 10,000 to 30,000 ft at a constant $M = 0.9$ for 17×17 modes with no flutter suppression system. The mode at 2 Hz is unstable for altitudes less than 24,000 ft. Figure 14 illustrates one of the results in which the gain of the suppression system, G, is varied from 0 to 14 at a constant altitude of 15,000 ft. The mode at 2 Hz now appears to be

Table 4 Coefficients of seventh-order polynomials (Mach number = 1.75)

Coef-ficient $d_{ij,n}$	Mode i	Mode j = 1 Real	1 Imaginary	2 Real	2 Imaginary
$d_{ij,0}$	1	−2.049320	0.0	0.0	0.0
	2	−2.252290	0.0	0.0	0.0
$d_{ij,1}$	1	−1.6102997	0.0	−1.9811527	0.0
	2	−1.5473675	0.0	−2.1963915	0.0
$d_{ij,2}$	1	−0.0908853	0.0	0.3092540	0.0
	2	−0.0819447	0.0	0.3374266	0.0
$d_{ij,3}$	1	0.0379471	0.0	−0.2727394	0.0
	2	0.0342803	0.0	−0.2657355	0.0
$d_{ij,4}$	1	−0.0112004	0.0	0.0924199	0.0
	2	−0.0102449	0.0	0.0893614	0.0
$d_{ij,5}$	1	0.0056365	0.0	−0.0509431	0.0
	2	0.0049488	0.0	−0.0464240	0.0
$d_{ij,6}$	1	−0.0006974	0.0	0.0062069	0.0
	2	−0.0006216	0.0	0.0057623	0.0
$d_{ij,7}$	1	0.0002991	0.0	−0.0027770	0.0
	2	0.0002559	0.0	−0.0024549	0.0

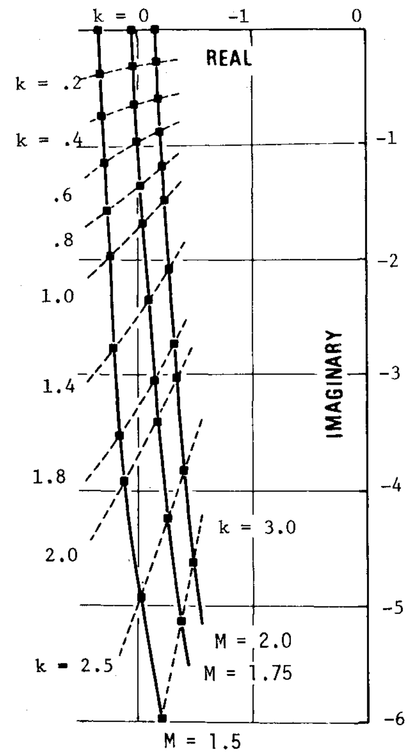

Fig. 11 q_{11} from lifting surface theory and from seventh-order polynomial approximation for $0 \leq k \leq 3.0^+$ and various supersonic Mach numbers.

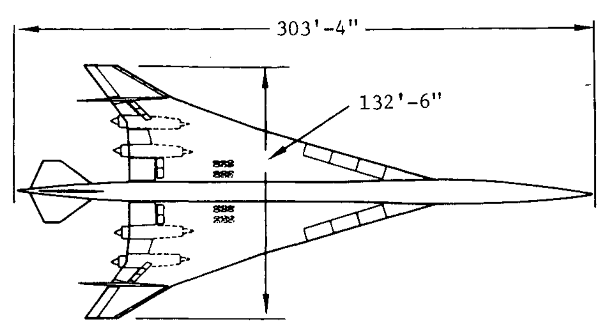

Fig. 12 Arrow wing SCAR configuration.

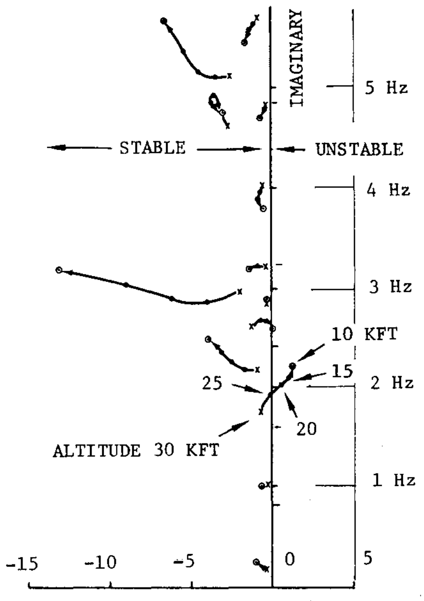

Fig. 13 Root loci due to altitude variation: Mach number = 0.9, modes = 17 × 17, altitude variation = 10,000 to 30,000 ft, flutter-suppression gain $G = 0$.

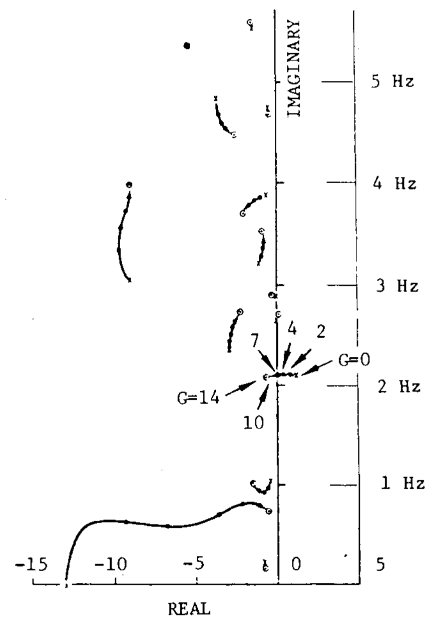

Fig. 14 Root loci due to gain variation: Mach number = 0.9, modes = 17 × 17, altitude = constant = 15,000 ft, gain variation = 0 to 14.

stable at $G = 7$. In this study, the applied polynomials are third-order in s with the least-squares approximation.

Concluding Remarks

A method of generating the reasonable approximations to aerodynamic transfer functions for general configurations of advanced elastic flight vehicles has been made.

The general solution of unsteady aerodynamic loadings of wings and wing-body combinations is represented by integral equations of the Fredholm types of the first and second kinds. The integral equation is, then, approximated by applying a finite-element concept which transforms the integral equation into a finite summation with the so-called aerodynamic influence coefficients. Therefore, one of the required conditions for the existence of a polynomial or rational function with respect to s is that the kernel of the integral equation is expandable with respect to k. The second requirement is that the modal functions of aircraft structures should be Riemann integrable.

Two types of power series approximation have been specified. One of these is a power series with real coefficients and the other is one with complex coefficients. From a practical point of view, the real coefficient power series method is applied in this study with either the standard data fit or the least-squares approximation fit.

From the study of characteristic behavior of unsteady aerodynamics in subsonic flow, there exists a hereditary effect of the wake on the wing-bound vortices. In this flowfield, by analogy to the feedback control system, the system loop is considered to be closed and either polynomials or rational functions can be used, but a form of the rational function which can be constructed by the Padé approximant method is believed to be best suited. In the supersonic flowfield, however, the system loop is opened and the appropriate form of transfer functions is polynomial. The extended Padé approximant, which transforms the origin into a certain value of ik_0 in which k_0 is a real value, is designed to improve the accuracy when k is large.In this extended case, however, the coefficients of the power series are no longer real values.

The program has been demonstrated for an AGARD wing in various flow Mach numbers of both the subsonic and supersonic flowfields. Determination of flutter instability boundaries for an advanced SCAR configuration to include active control surfaces driven by a flutter suppression system is also examined by applying this method. These computed results indicate that the method developed for evaluating the most reasonably approximate function of aerodynamic transfer functions in the frequency domain appears to provide satisfactory results.

This method can contribute significantly to both design knowledge and handling quality of aircraft, space shuttles, and associated systems – specifically in the area of stability and control, vibration and flutter, and problems related to the autopilot.

Acknowledgments

This paper summarizes work performed under the Boeing Aerospace Company Independent Research & Development under B.F. Dotson, Military Aircraft System Development. The author wishes to acknowledge the stimulating discussions held with M.J. Turner.

References

[1] Fung, Y.C., *Theory of Aeroelasticity*, Wiley, New York, 1955.

[2] Vepa, R., "Finite State Modeling of Aeroelastic Systems," Ph.D. Dissertation, Department of Aeronautics and Astronautics, Stanford University, Stanford, Calif., 1975.

[3] Hassig, H.J., "An Approximate True Damping Solution of the Flutter Equation by Determinant Iteration," *Journal of Aircraft*, Vol. 8, Nov. 1971, pp. 885 – 889.

[4] Hassig, H.J., "Approximate Aerodynamic Coefficients $A(k+ik)$ Obtained from $A(ik)$ by Polynomial Interpolation," presented at the Aerospace Flutter and Dynamic Council Meeting, Seattle, Wash., May 17-18, 1973.

[5] Dat, R., "Determination of the Dynamic Characteristics of Structures Using a Vibration Test with Point Excitation," La Recherche Aerospatiale, No. 1973 – 5, pp. 301 – 306.

[6] Vepa, R., "On the Use of Padé Approximants to Represent Unsteady Aerodynamic Loads for Arbitrarily Small Motions of Wings," AIAA Paper 76-17, AIAA 14th Aerospace Sciences Meeting, Washington, D.C., Jan. 26-28, 1976.

[7] Ashley, H. and Zartarian, G., "Piston Theory – A New Tool for the Aeroelastician," *Journal of Atmospheric Sciences*, Vol. 23, Dec. 1956, pp. 1109-1118.

[8] Baker, G.A., Jr., *Essentials of Padé Approximants*, Academic Press, New York, 1975.

[9] Ii, J.M., "Synthesis of Aerodynamic Transfer Functions for Advanced Elastic Flight Vehicles," AIAA Paper 77-452, San Diego, Calif., March 24-25, 1977.

[10]Rowe, W.S., Redman, M.C., Ehlers, F.E., and Sebastian, J.D., "Prediction of Unsteady Aerodynamic Loadings Caused by Leading Edge and Trailing Edge Control Surface Motions in Subsonic Compressible Flow-Analysis and Results," NASA CR-2543, Aug. 1975.

[11]Giesing, J.P., Kalman, T.P., and Rodden, W.P., "Subsonic Unsteady Aerodynamics for General Configurations," Pt. I, Vol. I; Direct Application of the Non-Planar Doublet Lattice Method, AFFDL-TR-71-5, Pt. I, Feb. 1971.

[12]Ii, J.M. and Tankerslay, D.F., "Unsteady Aerodynamic Interaction for Advanced Aircraft Configurations in Subsonic Flow (Improved Doublet Lattice Method, TEV 155)," Boeing Doc. D6-41258, Sept. 1973.

[13]Ii, J.M., and Borland, C.J., and Hogley, J.R., "Predictions of Unsteady Aerodynamic Loadings of Non-Planar Wings and Wing-Tail Configurations in Supersonic Flow,"Pt. I, Theoretical Development, Program Usage and Application, AFFDL-TR-71-108, March 1972.

[14]Ii, J.M. and Rowe, W.S., "Unsteady Aerodynamics of Non-Planar Wings and Wing-Tail Configurations of Elastic Flight Vehicles in Supersonic Flight," *Journal of Aircraft*, Vol. 10, Jan. 1973, pp. 19-27.

[15]Dreisbach, R.L., (ed.), "ATLAS-An Integrated Structural Analysis and Design System, User's Manual-Input and Execution Data," Boeing Doc. D6-25400-0003, March 1977.

[16]Hyland, F.G., "Review of SCAR Flutter Suppression System Study," Boeing Coordination Sheet (unpublished), Nov. 1976.